Nanoscale

Accepted Manuscript

This article can be cited before page numbers have been issued, to do this please use: J. P. Meng, Q. Li, J. Huang and Z. Li, *Nanoscale*, 2021, DOI: 10.1039/D1NR04752C.

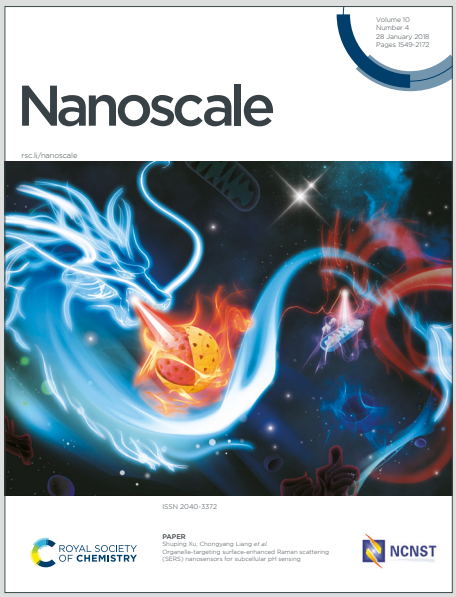

ROYAL SOCIETY OF CHEMISTRY

rsc.li/nanoscale

View Article Online
DOI: 10.1039/D1NR04752C

ARTICLE

Tunable Schottky barrier height of Pt-CuO junction via triboelectric nanogenerator

*Jianping Meng [a,b], Qi Li [a,d], Jing Huang [a,d], Zhou Li [a,b,c]**

Received 00th January 20xx,
Accepted 00th January 20xx

DOI: 10.1039/x0xx00000x

Tuning Schottky barrier height is crucial to optimize the performance of Schottky junction device. Here, we demonstrate that the Schottky barrier height can be tuned by the voltage from triboelectric nanogenerator (TENG). Schottky barrier heights at both ends are increased after the treatment of the voltage generated by TENG. The electric field generated by impulse voltage of TENG drives the diffusion of the ionized oxygen vacancy in CuO nanowire, which induces the nonuniform distribution of the ionized oxygen vacancy. The oxygen vacancy positively charged accumulates at the contacted interface of Pt and CuO nanowire, it impels the conduction and valence bands to bend downwards. The Schottky barrier height is raised. A theoretical model based on the energy band diagram is proposed to explain this phenomenon. This method offers a simple and effective avenue to tune the Schottky barrier height. It opens up the possibility to develop the high Schottky sensor by tuning the Schottky barrier height.

Introduction

Schottky contact is an important role in virtually all micro-electric fields. Schottky barrier height at the interface of metal-semiconductor controls the depletion width and the mechanism of carrier transport.[1, 2] Tuning Schottky barrier height can optimize the performance of Schottky devices. [3, 4] By tuning Schottky barrier height, the detecting performance is significantly enhanced for photodetector,[5-7] gas sensor,[8, 9] biosensor,[10-12] chemical sensor,[13] strain sensor,[14] and so on.

Piezotronic effect as a dynamic adjusting method of Schottky barrier height is an effective way for piezoelectric semiconductors (including ZnO, GaN, ZnS, CdS, and so on) once a stress is applied.[15-17] Then, the transport process of the carrier is modulated at the interface/junction.[18] Piezotronic effect has been utilized to develop the high-performance sensor based on Schottky contact.[16] The piezoelectric semiconductor with nanowire structure allows the large deformations before fracture comparing with bulk materials. However, the risk of fracture is increased after multiple deformations in process of the experiment. Another dynamic adjusting method is the polarization of charged oxygen vacancy in ZnO nanowire (n-type) using triboelectric nanogenerator (TENG) with the properties of high voltage and low current.[19-21] The discovery that the Schottky barrier height of the Ag-ZnO junction is decreased after being treated by TENG is noticeable.[5, 9, 11, 22] Whereas the change of Schottky barrier height based on p-type nanowire semiconductor after being treated by TENG is still needed to investigate to understand this effect in-depth. CuO nanowire has been known as a p-type semiconductor that exhibits a narrow bandgap and other interesting properties [23, 24]. CuO nanowire is a promising p-type semiconductor due to its easy fabrication, low cost, environmentally friendly nature, and easy preparation. Schottky junction based on CuO nanowire is widely applied in the field of photodetector,[25-27] gas detection,[28, 29] chemical sensor,[30] memristors,[31] field-effect transistors,[32] and so on.

In this work, we chose CuO nanowire as a p-type semiconductor to prepare a device of the Schottky junction. The high voltage produced by TENG is used to modulate Schottky barrier height. The phenomenon that Schottky barrier height of Pt and CuO nanowire is increased after treatment by TENG. A

a CAS Center for Excellence in Nanoscience, Beijing Key Laboratory of Micro-nano Energy and Sensor, Beijing Institute of Nanoenergy and Nanosystems, Chinese Academy of Sciences, Beijing, 101400, China
b School of Nanoscience and Technology, University of Chinese Academy of Sciences, Beijing 100049, P. R. China
c Center on Nanoenergy Research, School of Physical Science and Technology, Guangxi University, Nanning 530004, P.R. China
d College of Chemistry and Chemical Engineering, Guangxi University, Nanning, 530004, China

theoretical model is proposed to explain this phenomenon. The discovery in this work is beneficial to understand the interaction mechanism between impulse voltage of TENG and Schottky barrier height. It provides an avenue to develop high-performance Schottky-contacted sensors.

Experimental

Materials preparation and characterization: CuO nanowires were synthesized by heating copper substrate in air according to the protocol of Jiang *et al.*.[33] The surface morphology of CuO nanowire was obtained by scanning electron microscope (SEM, Hitachi SU8020). X-ray diffraction (XRD) pattern was used to get the information of phase structure by X-ray diffractometer (PANalytical X`Pert) with Cu kα source (λ=0.154 nm). Composition and microstructure of were investigated by transmission electron microscope (TEM, Tecnai G^2 F20) equipped with a high-angle angular-dark-field detector and X-ray energy-dispersive spectrometer systems.

Fabrication of TENG and Schottky junction: A 4-mm acrylic plate served as the robust substrate. Aluminum foil and Kapton membrane were chosen as friction layers to generate high voltage. The size of aluminum foil and Kapton film is 8 cm × 8 cm. The Cu film with the thickness of 50 nm was deposited on the back side of Kapton film with the thickness of 100 μm is used as the electrode. Copper electrodes with a spacing of 10 μm were deposed on the substrate of amorphous SiO_2 by UV-lithography technology. CuO nanowires were ultrasonically dispersed in ethanol. CuO nanowires were aligned on the Cu electrode array by electric-field assisted assembly and alignment. The voltage of 12 V with the frequency of 50 kHz is generated by the signal generator (ArbStudio 1104) to produce an alternating electric field. Pt electrode was deposited on both sides of CuO nanowires by the technology of focus ion beam (FIB, FEI Scios 2) to form Schottky contact.

Electrical Measurements: Voltage of TENG was measured by Tektronix oscilloscope (Type: HD06104). *I-V* curve ranged from -5 V to 5 V was recorded by semiconductor characterization system (Keithley 4200-SCS).

Results and discussion

CuO nanowire is synthesized by the vapor-solid method. It is grown by heating a copper grid in air. Copper gride used in transmission electron microscopy is cleaned in an aqueous 1.0 M HCl solution for ~20 s. Afterward, it was rinsed with distilled water repeatedly, following by drying under a N_2 gas flow. Copper gride was heated for 10 h in a tube furnace with a temperature of 500 ºC immediately (Figure 1a-d). CuO nanowires with the length ranged from 10 μm to 30 μm are obtained (Figure 1e). XRD pattern indicates that CuO nanowires are composed of CuO and Cu_2O. When copper gride is heated in air, the major product is Cu_2O. CuO is synthesized slowly through the oxidation of Cu_2O further. In this case, Cu_2O is the precursor to the formation of CuO. The formation of CuO vapor from Cu_2O is rate-determining step [33].

$$4Cu + O_2 \rightarrow 2Cu_2O \quad (1)$$

$$2Cu_2O + O_2 \rightarrow 4CuO \quad (2)$$

Vapor pressure for CuO in the chamber is low due to the slow rate for the formation of CuO. It ensures a continuous growth mode and uniform diameter for the CuO nanowires. Additionally, the slow growth rate is beneficial to improve the crystallinity of CuO nanowire.

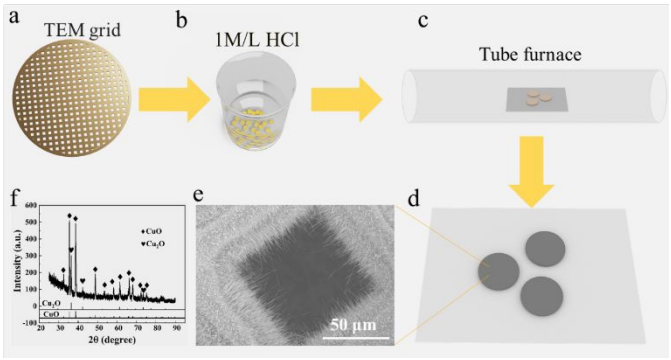

Figure 1. Synthesis steps and characterization of CuO nanowire. (a-d) The synthesis process of CuO nanowires. (e) SEM image of CuO nanowires. (f) XRD pattern of CuO nanowires.

TEM method is utilized to characterize the morphology and microstructure further. The diameter of prepared CuO nanowires is about 150 nm (Figure 2a). The regular arrangement of atoms observed from high-resolution TEM (HRTEM) image exhibits the nature of high crystallinity (Figure 2b). Fluctuation in the arrangement of the atoms is owing to slight stacking faults in CuO nanowires. The interplanar distances measured from the HRTEM image are 2.496 Å, 2.306 Å, 2.275 Å, respectively, which are assigned to the panels of $(\bar{1}11)$, (111), and (200) in the CuO nanowires. The two sets of diffraction spots are observed in the SAED image (Figure

View Article Online
DOI: 10.1039/D1NR04752C

2c) confirming the existence of stacking faults within the CuO nanowire. The calibration of diffraction spots is corresponding to the diffraction of the lattice plane in CuO. EDS spectrum of a single CuO nanowire is shown as the red (Cu) and green (O) color (Figure 2e-f). The clear signal of Cu and O elements is further evidence of CuO nanowire.

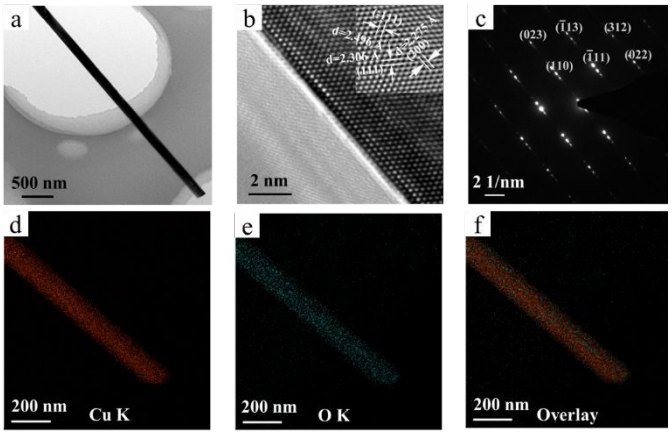

Figure 2. Structural information of CuO nanowire. (a-c) TEM image, HRTEM, and SAED image of CuO nanowire. (d-f) EDS element mappings of Cu, O.

The voltage of TENG after rectification is applied on Pt-CuO-Pt Schottky diode (Figure 3a). The corresponding equivalent circuit is shown in figure 3b. R_{nw} is the resistance of nanowire. R_{sh1} and R_{sh2} are the shunt resistances associated with the two Schottky barriers [34, 35]. The output voltage of TENG after rectification is about 180 V with a frequency of 1 Hz (Figure 3c). The device exhibits the non-linear *I-V* curve, which indicates the Schottky junction is formed between Pt and CuO nanowire at both ends (Figure 3d). The almost symmetrical *I-V* curve infers the approaching Schottky barrier height. The inset image at the top of figure 3d is the SEM image of the Pt-CuO-Pt Schottky diode. The almost same area of Pt and uniform performance of CuO nanowire makes the formation of approaching Schottky barrier height. According to the classic thermionic emission-diffusion theory ($V>>3kT/q$~77 mV) ,[36, 37] the current of the Schottky diode can be determined as follow formulae

$$I_R = SA^*T^2 \exp(-\frac{\phi_{B0}}{kT}) \exp\left(\frac{\sqrt[4]{q^7 N_D (V + V_{bi} - kT/q)/(8\pi^2 \varepsilon_s^3)}}{kT}\right) \quad (1)$$

in which S is the contact area between metal and semiconductor, A^* is the effective Richardson constant, the value is 14.5 A/cm^{2}K^2,[38] T is the absolute temperature, ϕ_{B0} is the Schottky barrier height, k is the Boltzmann constant, q is the unit electronic charge, N_D is the doping concentration, V is the applied voltage, V_{bi} is the build-in potential, ε_s is the permittivity of CuO. The Schottky barrier height is obtained by plotting the curve of ln (*I*) and $V^{1/4}$. Schottky barrier heights of drain and source are 0.56 and 0.55 eV after calculation. The inset image at the bottom of figure 3d is a schematic of the Pt-CuO-Pt Schottky diode.

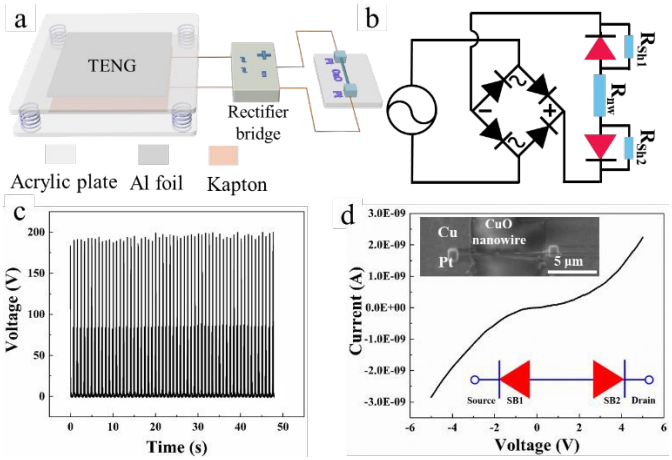

Figure 3. Diagram of experiment setup and basic performance of TENG and Pt-CuO-Pt Schottky device. (a) Schematic illustration of the experiment setup. (b) equivalent circuit corresponding to the figure a. (c) Open-circuit voltage of TENG. (d) *I-V* curve of Pt-CuO-Pt Schottky device, the inset on the top is the SEM image of Pt-CuO-Pt, the inset on the bottom is the schematic structure of the device.

I-V curve before and after TENG treatment is shown in Figure 4a. The current of the Pt-CuO-Pt Schottky diode is decreased after TENG treatment, additionally, the decrease amount is enhanced with the increase of treatment times. Schottky barrier heights of source and drain are raised from 0.55 and 0.56 eV to 0.59 and 0.60 eV (Figure 4b). Schottky barrier height increases monotonously by increasing times of TENG treatment. When Pt and CuO nanowire are contacted, the Schottky barrier (hole barrier) is formed because of (i) the difference of the work function of Pt and the ionization energy of CuO nanowire, and (ii) surface state of CuO nanowire (Figure 4c). The conduction and valence bands bend downwards. The Schottky barrier height is increased after the treatment by the voltage from TENG (Figure 4d). It is well known that the native oxygen defect is generated inevitably during the synthetic process of CuO nanowires because of low formation energy [26]. It is showed as the black spheres in the atomic structure of CuO (Figure 4c). Defect in CuO nanowire

creates defect localized states. The interaction of the external electric field and localized state around the oxygen defect happens once the electric field is applied. Electrical potential induced by the external electrical field will be proportionally and directly converted into energy gain in CuO nanowires associated with local lattice relaxations. Oxygen vacancy is charged under the stimulation of electric field from the out-put voltage of TENG. It converts into ionized oxygen vacancy ($V_O^0 \rightarrow e + V_O^+$ or $V_O^+ \rightarrow e + V_O^{2+}$).[39, 40] Ionized oxygen vacancies are diffused toward the interface of Pt and CuO nanowire. The ionized oxygen vacancy with positive charge accumulated at the interface.[41] It acts as the positive "gate" voltage, which leads to the conduction and valence bands of CuO around the interface bend downwards simultaneously. The Schottky barrier height formed by Pt and CuO nanowire is raised.

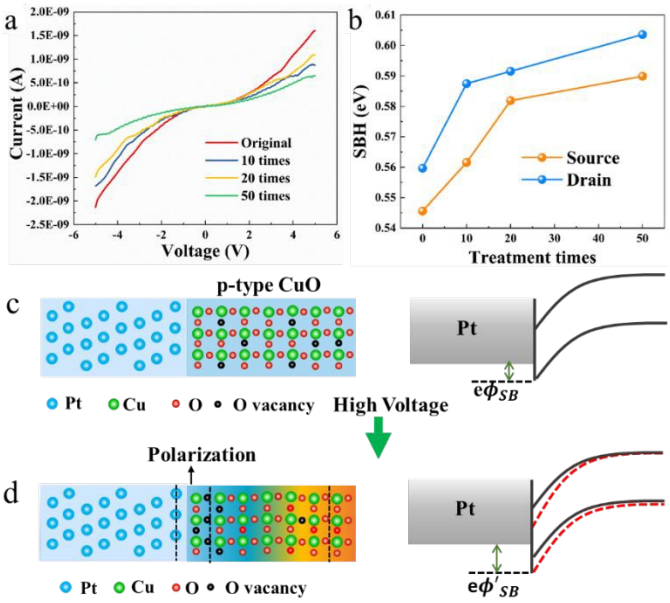

Figure 4. Change of Schottky barrier height and polarization model of Pt and CuO (p-type) interface to Pt-CuO-Pt. (a) *I-V* curves of the Pt-CuO-Pt device under different times of TENG treatment. (b) the corresponding change of Schottky barrier height at source and drain. (c) Schematic atomic structure of the Pt-CuO device, band diagram of Schottky contacted Pt-CuO (p-type) interface at initial state. (d) The oxygen vacancies are driven by the positive high voltage of TENG, and they are accumulated at the junction around the interface.

Conclusions

In summary, we investigate the influence of impulse voltage of TENG on the Schottky barrier height of Pt-CuO-Pt. First, the uniform CuO nanowires (~150 nm in diameter) with lengths ranged from 10 to 30 μm is synthesized by the vapor-solid method. The stacking fault is found in CuO nanowire by analysis of HRTEM and SAED. Then, the Schottky-contacted device based on CuO nanowires and Pt is fabricated by electric-field assisted alignment and focus ion beam technology. The interaction of the output voltage from TENG and CuO nanowire-based Schottky junction is investigated. The Schottky barrier height is raised after the treatment by the voltage of TENG. A theoretical model based on the energy band diagram is proposed to explain the phenomenon of the change of Schottky barrier height. The oxygen vacancy is transferred into the ionized oxygen vacancy under the impact of voltage from TENG. The ionized oxygen vacancy is diffused toward the contact interface of Pt and CuO nanowire, which leads to the increase of Schottky barrier height. This work is beneficial to understand the tuning effect of Schottky barrier height in depth. This method opens up the possibility to develop a high-performance Schottky sensor by modulating Schottky barrier height.

Author contributions

Jianping Meng: Conceptualization, investigation, methodology, writing-original draft, data curation, validation, funding acquisition. Qi Li: Investigation, data curation. Jing Huang: Investigation. Zhou Li: Supervision, resources, funding acquisition, writing - review & editing. All authors writing-review & editing.

Conflicts of interest

There are no conflicts to declare.

Acknowledgements

The authors are thankful for the support provided by the Beijing Natural Science Foundation (2214083, JQ20038), the National Natural Science Foundation of China (52002027, T2125003, 61875015), and the Youth Backbone Individual Project of Beijing Excellent Talents Training (Y9QNGG0501).

References

1. R. T. Tung, *Mat Sci Eng R*, 2001, **35**, 1-138.
2. J. P. Meng and Z. Li, *Adv Mater*, 2020, **32**, 2000130.

3. R. Yu, S. Niu, C. Pan and Z. L. Wang, *Nano Energy*, 2015, **14**, 312-339.
4. C. F. Pan, J. Y. Zhai and Z. L. Wang, *Chem Rev*, 2019, **119**, 9303-9359.
5. H. Li, L. M. Zhao, J. P. Meng, C. F. Pan, Y. Zhang, Y. M. Zhang, Z. Liu, Y. Zou, Y. B. Fan, Z. L. Wang and Z. Li, *Nano Today*, 2020, **33**.
6. Z. Yang, M. Jiang, L. Guo, G. Hu, Y. Gu, J. Xi, Z. Huo, F. Li, S. Wang and C. Pan, *Nano Energy*, 2021, **85**, 105951.
7. F. Yang, M. L. Zheng, L. Zhao, J. M. Guo, B. Zhang, G. Q. Gu, G. Cheng and Z. L. Du, *Nano Energy*, 2019, **60**, 680-688.
8. N. Simiao, H. Youfan, W. Xiaonan, Z. Yusheng, Z. Fang, L. Long, W. Sihong and W. Z. Lin, *Adv Mater*, 2013, **25**, 3701-3706.
9. J. P. Meng, H. Li, L. M. Zhao, J. F. Lu, C. F. Pan, Y. Zhang and Z. Li, *Nano Lett*, 2020, **20**, 4968-4974.
10. P. H. Yeh, Z. Li and Z. L. Wang, *Adv Mater*, 2009, **21**, 4975-4978.
11. L. M. Zhao, H. Li, J. P. Meng, A. C. Wang, P. C. Tan, Y. Zou, Z. Q. Yuan, J. F. Lu, C. F. Pan, Y. B. Fan, Y. M. Zhang, Y. Zhang, Z. L. Wang and Z. Li, *Adv Funct Mater*, 2020, **30**, 1907999.
12. R. Yu, C. Pan, J. Chen, G. Zhu and Z. L. Wang, *Adv Funct Mater*, 2013, **23**, 5868-5874.
13. C. Pan, R. Yu, S. Niu, G. Zhu and Z. L. Wang, *ACS Nano*, 2013, **7**, 1803-1810.
14. Z. Zhang, Q. L. Liao, X. H. Zhang, G. J. Zhang, P. F. Li, S. N. Lu, S. Liu and Y. Zhang, *Nanoscale*, 2015, **7**, 1796-1801.
15. Z. L. Wang, *J Phys Chem Lett*, 2010, **1**, 1388-1393.
16. Z. L. Wang and W. Z. Wu, *Nat Sc Rev*, 2014, **1**, 62-90.
17. W. Z. Wu and Z. L. Wang, *Nat Rev Mater*, 2016, **1**.
18. Z. L. Wang, W. Z. Wu and C. Falconi, *Mrs Bull*, 2018, **43**, 922-927.
19. H. F. Qin, G. Q. Gu, W. Y. Shang, H. C. Luo, W. H. Zhang, P. Cui, B. Zhang, J. M. Guo, G. Cheng and Z. L. Du, *Nano Energy*, 2020, **68,** 10432.
20. L. Zhao, K. Chen, F. Yang, M. L. Zheng, J. M. Guo, G. Q. Gu, B. Zhang, H. F. Qin, G. Cheng and Z. L. Du, *Nano Energy*, 2019, **62**, 38-45.
21. M. L. Zheng, F. Yang, J. M. Guo, L. Zhao, X. H. Jiang, G. Q. Gu, B. Zhang, P. Cui, G. Cheng and Z. L. Du, *Nano Energy*, 2020, **73,** 104808.
22. L. M. Zhao, H. Li, J. P. Meng, Y. Zhang, H. Q. Feng, Y. X. Wu and Z. Li, *Sci Bull*, 2021, **66**, 1409-1418.
23. A. Tombak, M. Benhaliliba, Y. S. Ocak and T. Kilicoglu, *Results Phys*, 2015, **5**, 314-321.
24. C. Florica, A. Costas, A. G. Boni, R. Negrea, L. Ion, N. Preda, L. Pintilie and I. Enculescu, *Appl Phys Lett*, 2015, **106**.
25. P. Wang, X. H. Zhao and B. J. Li, *Opt Express*, 2011, **19**, 11271-11279.
26. L. B. Luo, X. H. Wang, C. Xie, Z. J. Li, R. Lu, X. B. Yang and J. Lu, *Nanoscale Res Lett*, 2014, **9**, 1-8.
27. T.-Y. Wei, C.-T. Huang, B. J. Hansen, Y.-F. Lin, L.-J. Chen, S.-Y. Lu and Z. L. Wang, *Appl Phys Lett*, 2010, **96**, 013508.
28. S. Steinhauer, E. Brunet, T. Maier, G. C. Mutinati, A. Kock, O. Freudenberg, C. Gspan, W. Grogger, A. Neuhold and R. Resel, *Sens Actuators B*, 2013, **187**, 50-57.
29. L. Liao, Z. Zhang, B. Yan, Z. Zheng, Q. L. Bao, T. Wu, C. M. Li, Z. X. Shen, J. X. Zhang, H. Gong, J. C. Li and T. Yu, *Nanotechnology*, 2009, **20**.
30. D. D. Li, J. Hu, R. Q. Wu and J. G. Lu, *Nanotechnology*, 2010, **21**.
31. Z. Fan, X. D. Fan, A. Li and L. X. Dong, *Nanoscale*, 2013, **5**, 12310-12315.
View Article Online
DOI: 10.1039/D1NR04752C
32. B. J. Hansen, N. Kouklin, G. H. Lu, I. K. Lin, J. H. Chen and X. Zhang, *J Phys Chem C*, 2010, **114**, 2440-2447.
33. X. C. Jiang, T. Herricks and Y. N. Xia, *Nano Lett*, 2002, **2**, 1333-1338.
34. Z. Y. Zhang, K. Yao, Y. Liu, C. H. Jin, X. L. Liang, Q. Chen and L. M. Peng, *Adv Funct Mater*, 2007, **17**, 2478-2489.
35. Y. Liu, Z. Y. Zhang, Y. F. Hu, C. H. Jin and L. M. Peng, *J Nanosci Nanotechno*, 2008, **8**, 252-258.
36. K. K. N. S. M. Sze, *New York, NY*, 1981.
37. J. Zhou, Y. D. Gu, P. Fei, W. J. Mai, Y. F. Gao, R. S. Yang, G. Bao and Z. L. Wang, *Nano Lett*, 2008, **8**, 3035-3040.
38. R. Jana, S. Sil, A. Dey, J. Datta and P. P. Ray, *Aip Adv*, 2018, **8**.
39. S. Lany and A. Zunger, *Phys Rev B*, 2005, **72**, 035215.
40. B. L. Huang, M. Z. Sun and D. F. Peng, *Nano Energy*, 2018, **47**, 150-171.
41. Y. Ding, Y. Liu, S. M. Niu, W. Z. Wu and Z. L. Wang, *J Appl Phys*, 2014, **116**, 154304.